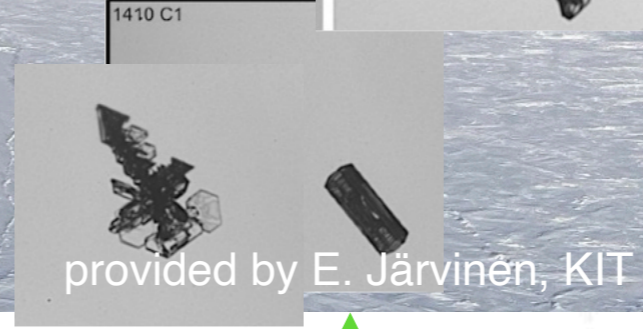
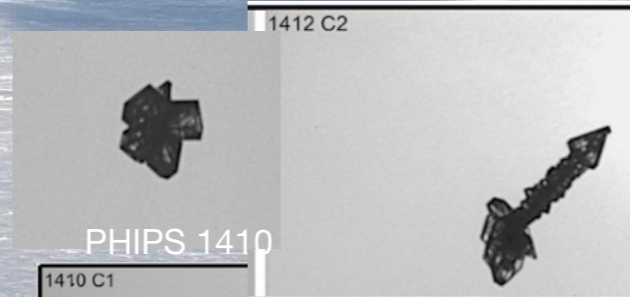


14:09UTC

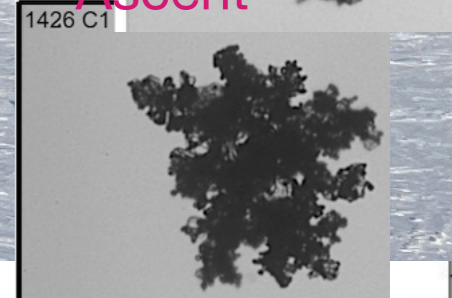
**First detected particles (by Nevzorov, PHIPS)
already appear to be ice, growth by vapor diffusion**

@ 160 m

2DS Ice conc ~ 20/L



Ascent



provided by E. Järvinen, KIT

WCR

13:50

13:55

14:00

14:05

14:10

14:15

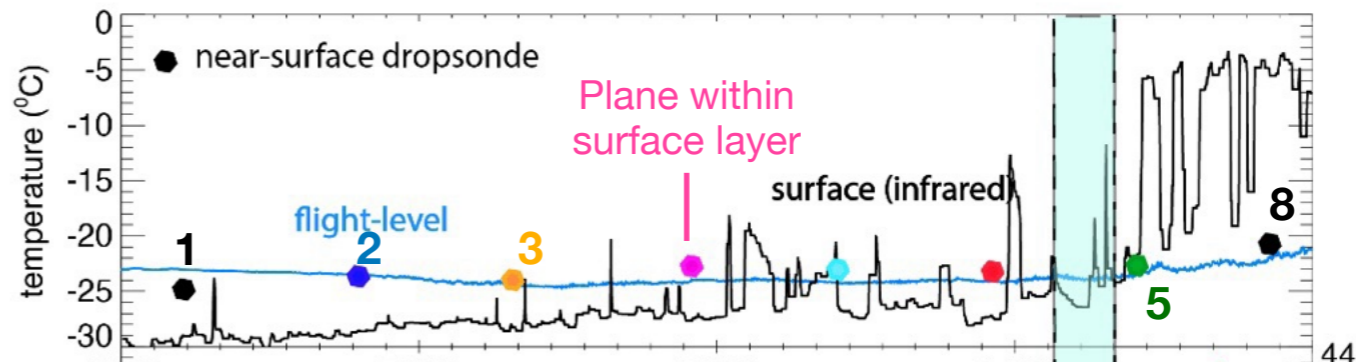
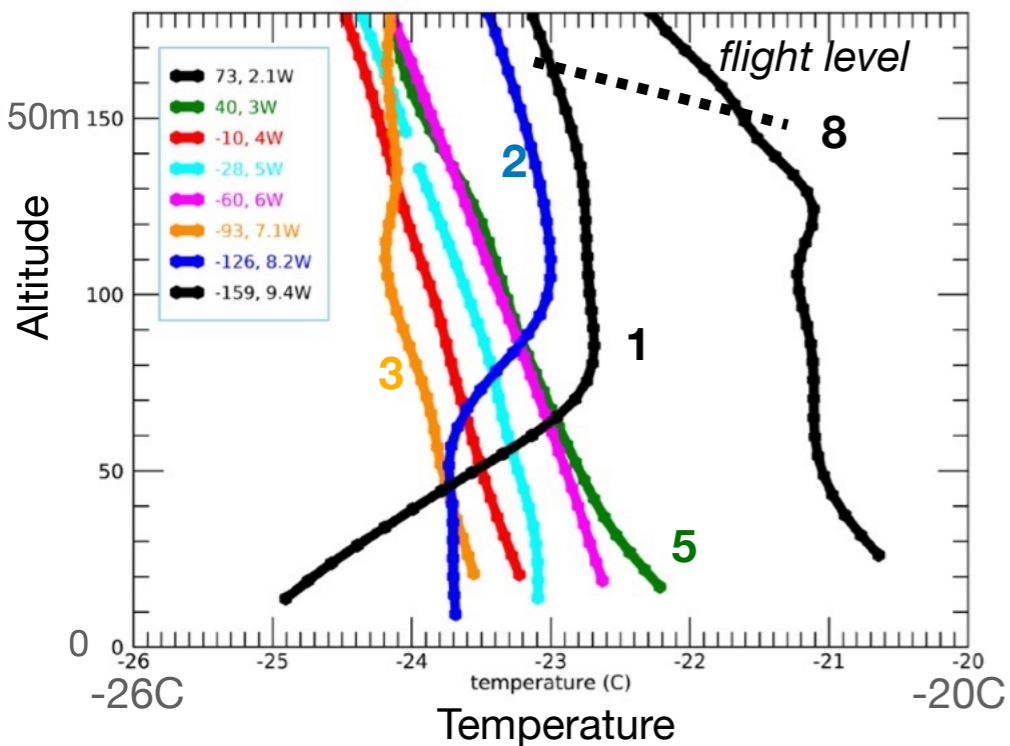
14:20

14:25

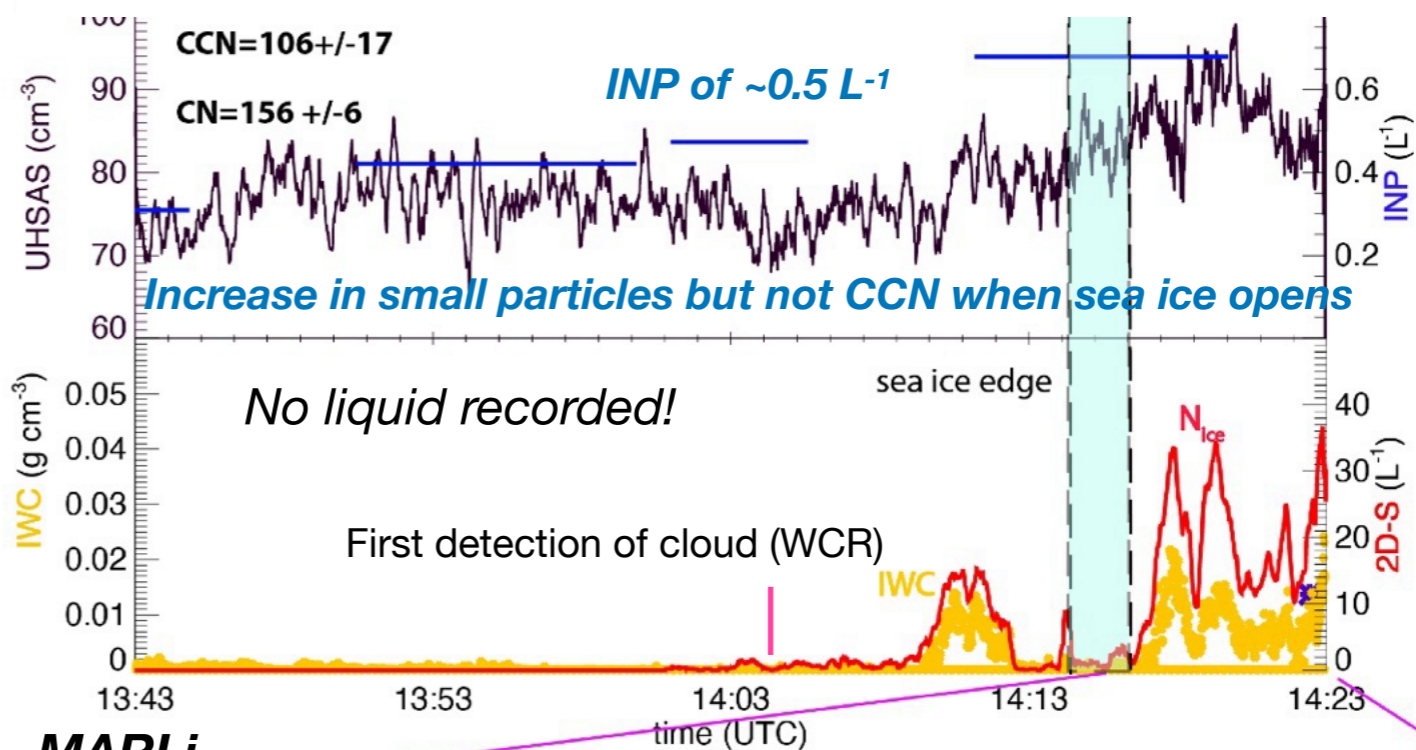


Dropsonde profiles along transit out above sea ice

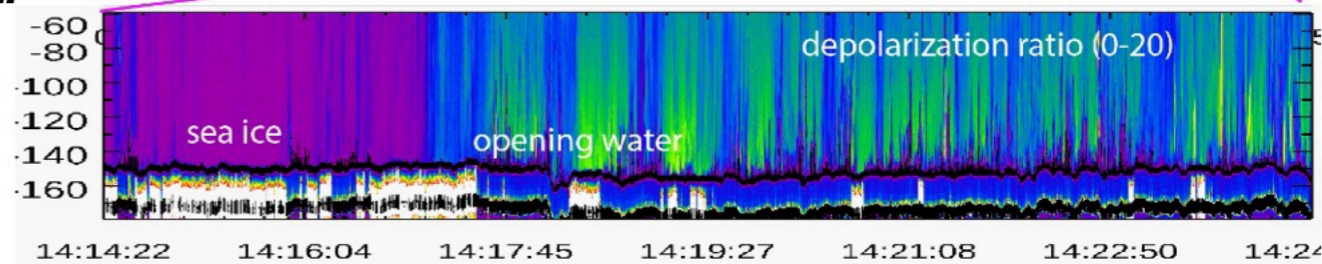
March 16



Furthest west



MARLi

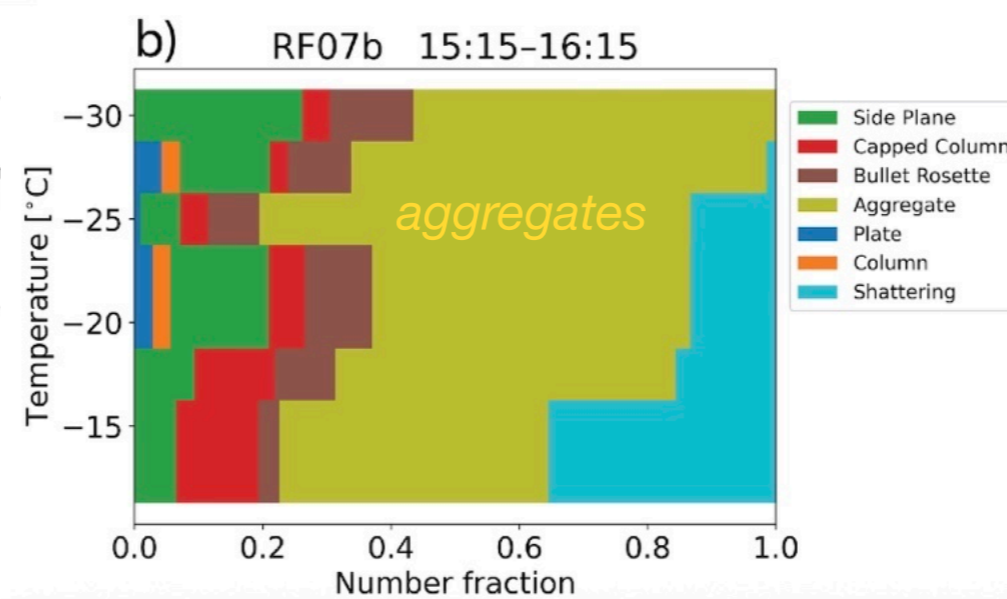
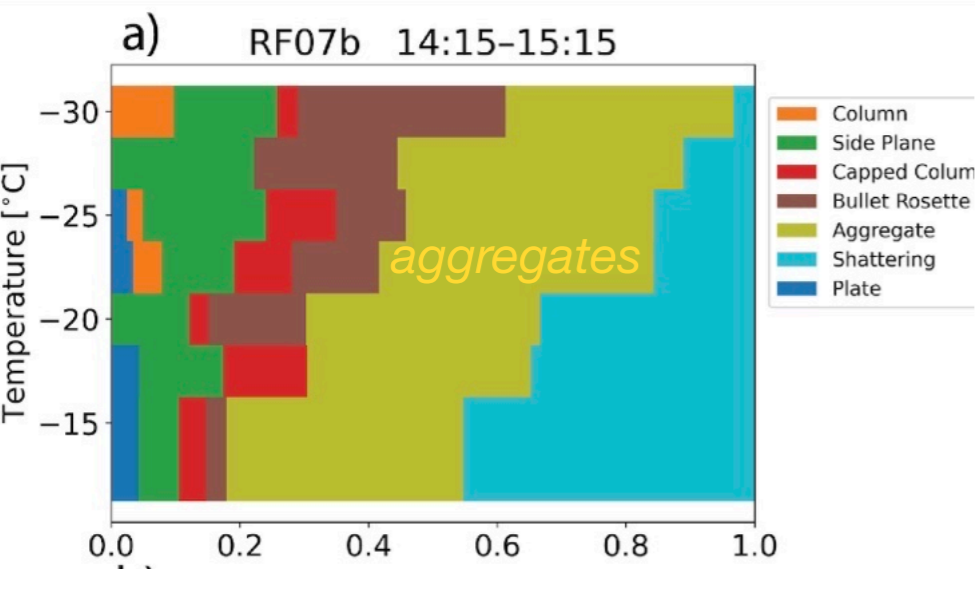
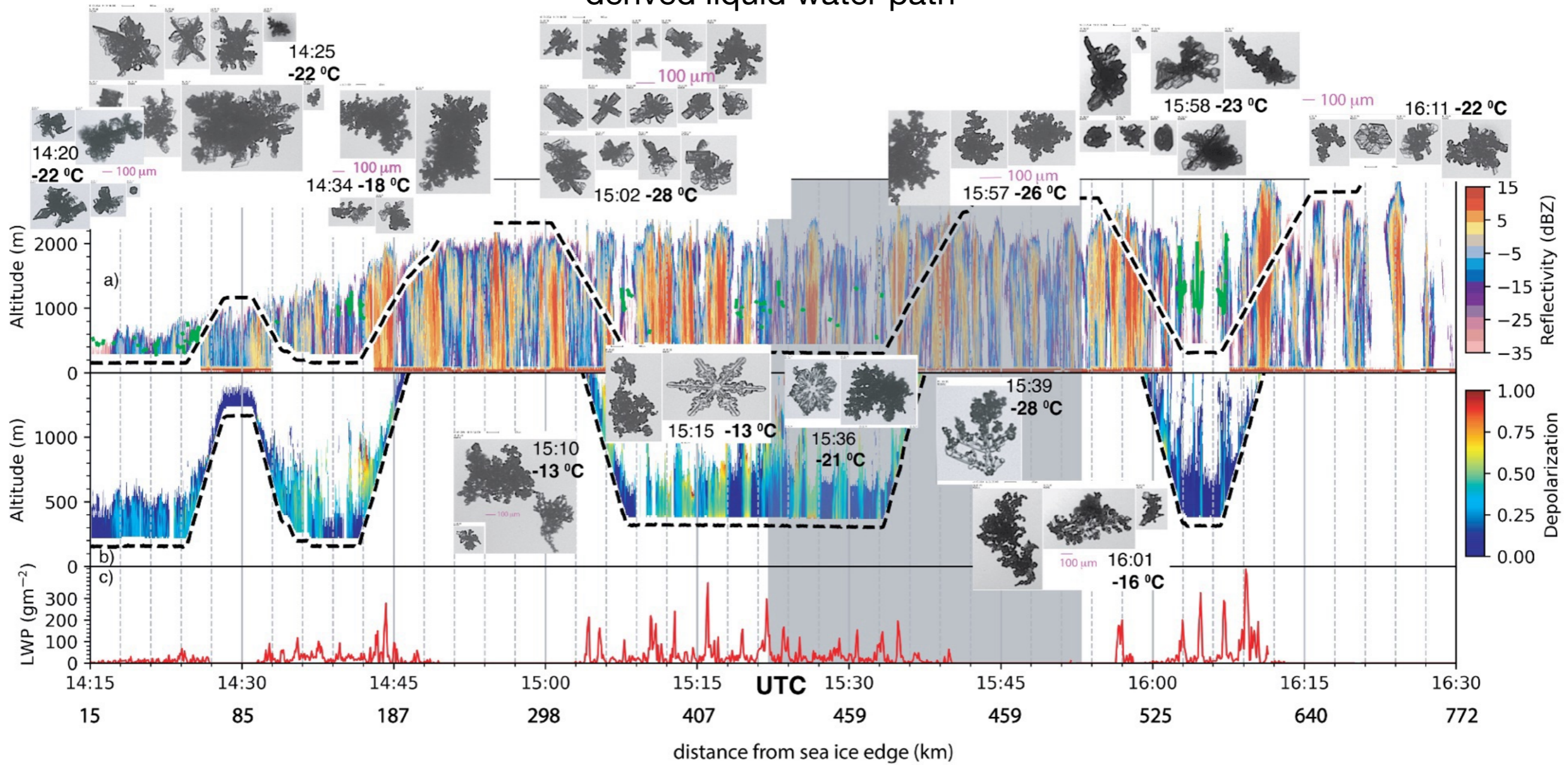


Ice particles appear to originate from near-instantaneous condensation+freezing at -25C over leads

13:40 UTC

~ 250 km

a) up+down pointing 95 GHz radar+PHIPS microphysical imagery; b) lidar depolarization; c) microwave-derived liquid water path



Emma Jarvinen habit-characterization analysis indicates more aggregates with fetch (riming not considered)

This CAO morphed into a polar low near Norway....strongly convectively driven, cloud tops went from 2.5 km to 4km. weak low-level baroclinicity+ upper-level potential vorticity anomaly
 (On-going analysis by Pablo Velt/Bart Geerts)

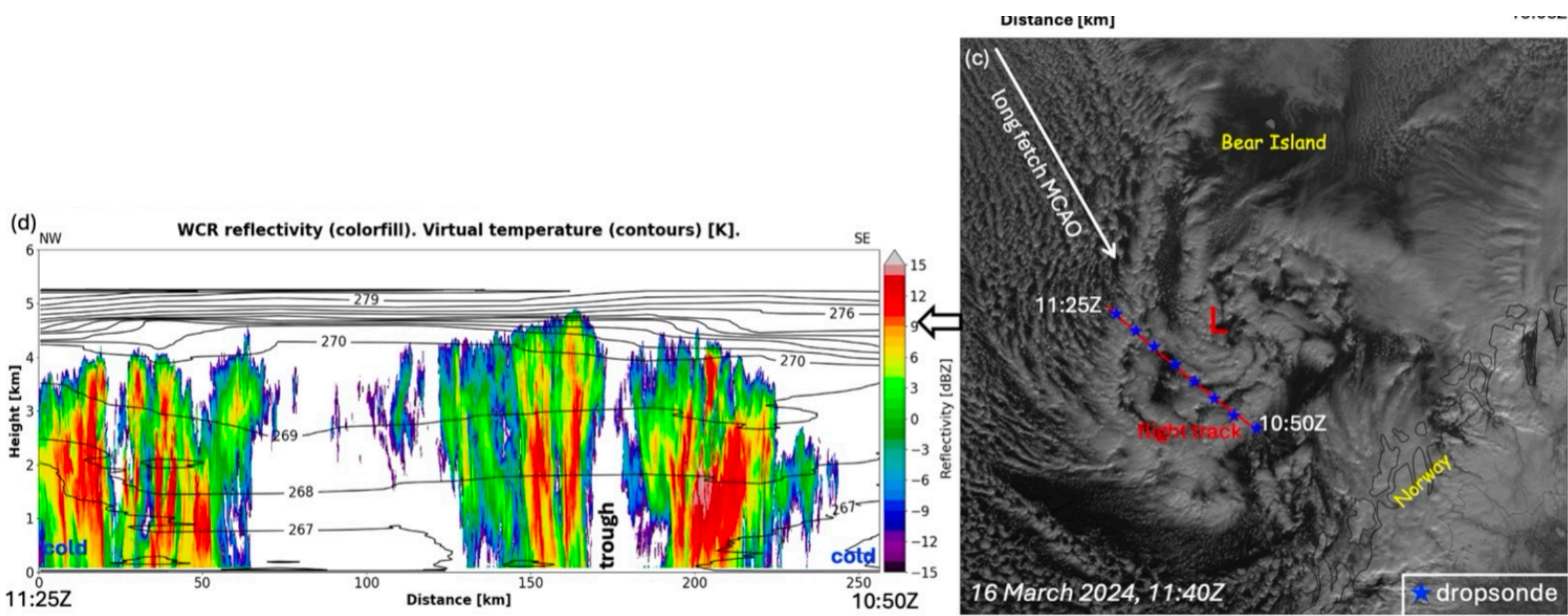
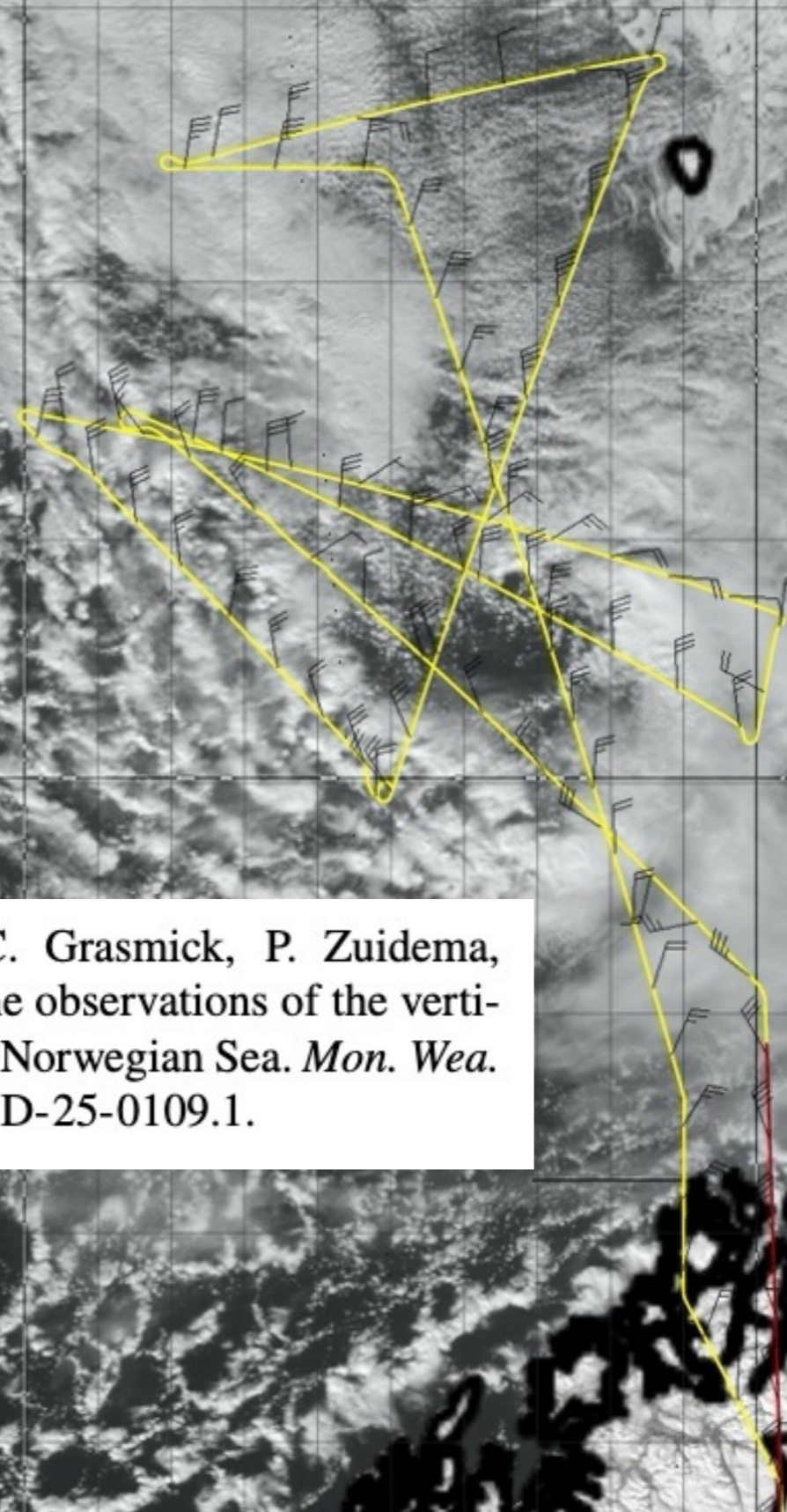
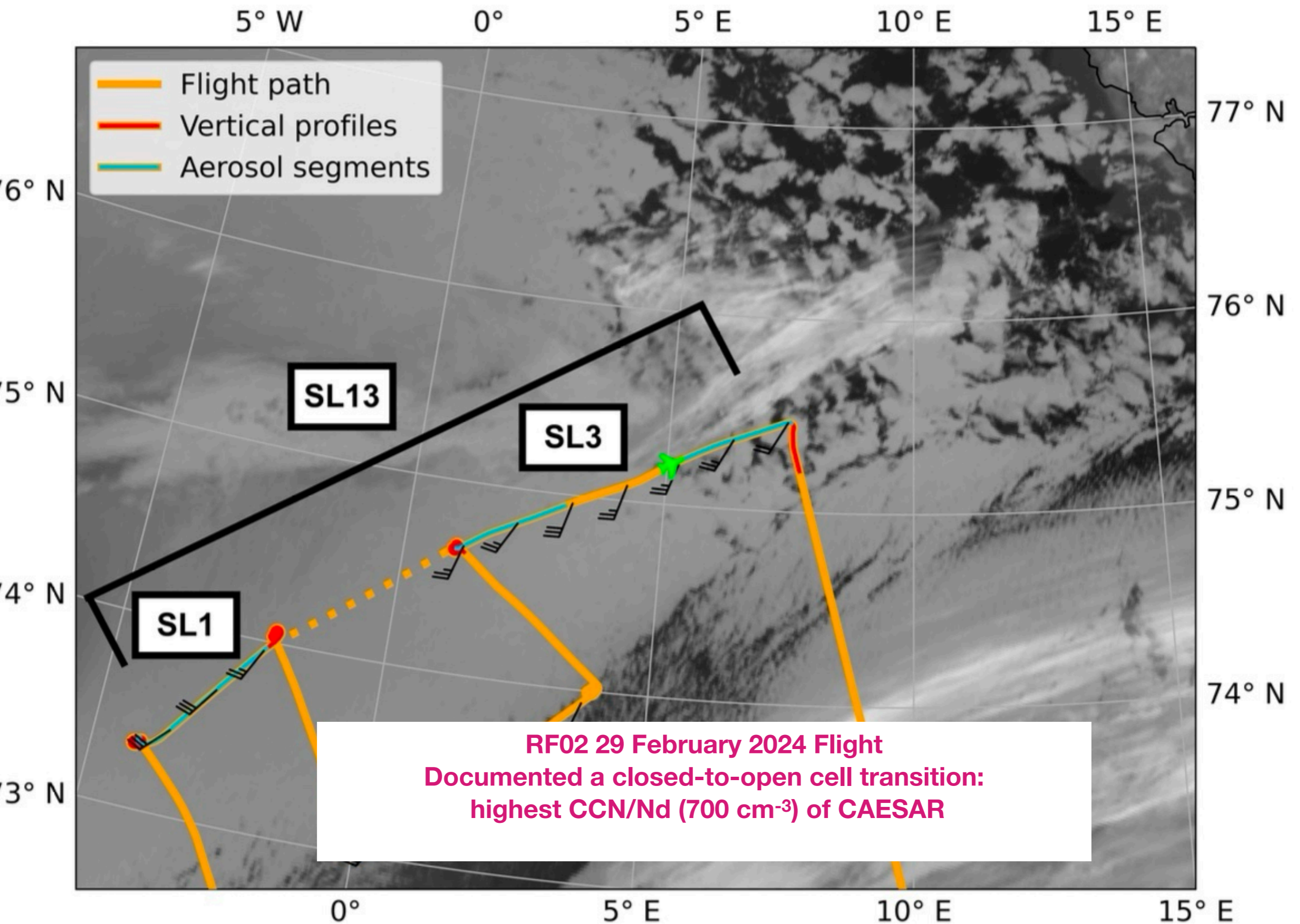


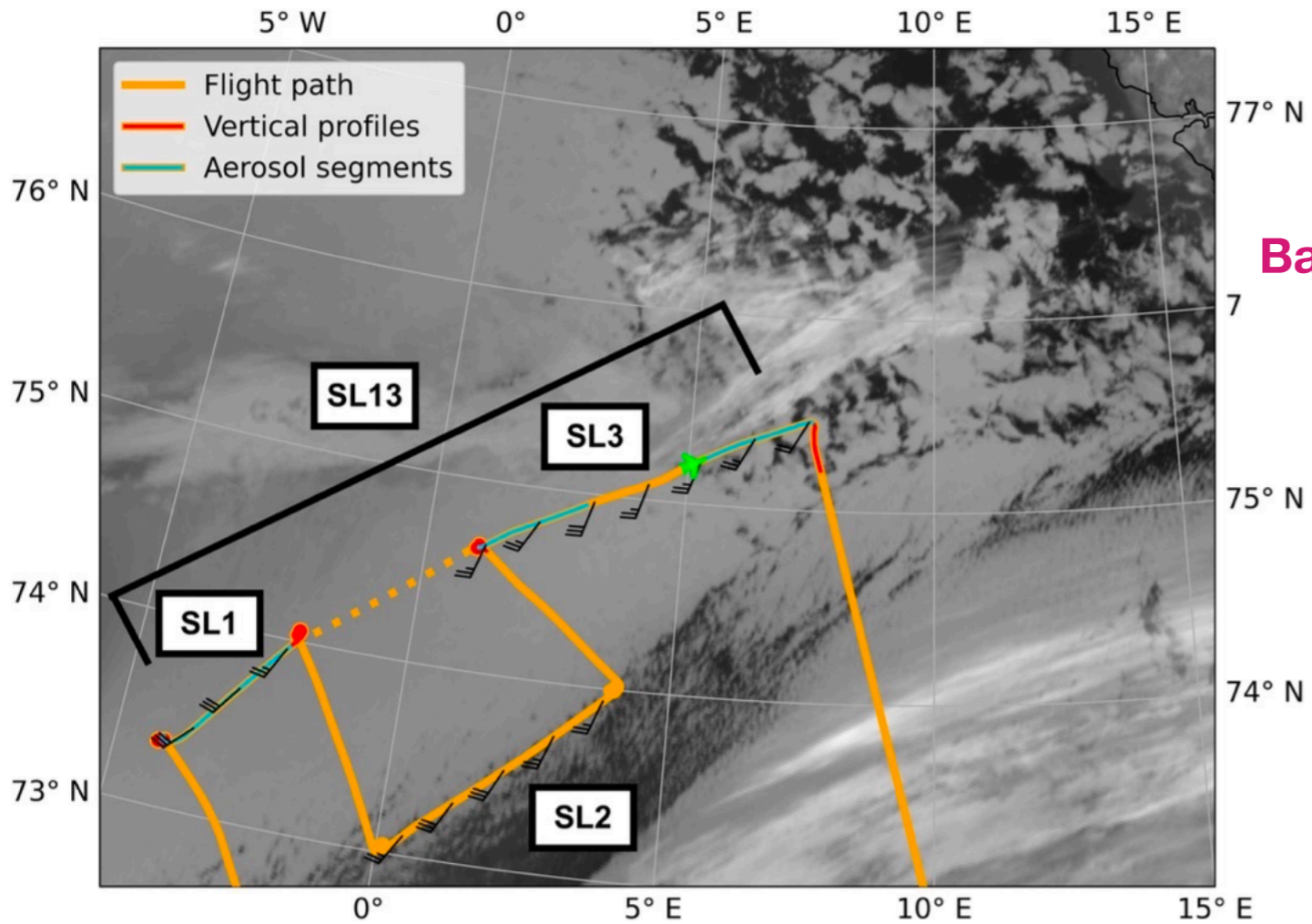
FIG. 9. Two polar lows, a shallow system sampled on 2 April (RF09; panels a-b) and a deeper, more convective polar low on 16 March (RF07; panels c-d). a) Advanced Very High Resolution Radiometer (AVHRR) visible image on 2 April 12:40 UTC (RF09), with C-130 flight track shown from 14:15 UTC to 15:05 UTC (dotted line). b) RF09 2 April 14:15 UTC-15:05 UTC WCR reflectivity with aircraft track shown colored by the

Polar cyclogenesis
2 April, RF09

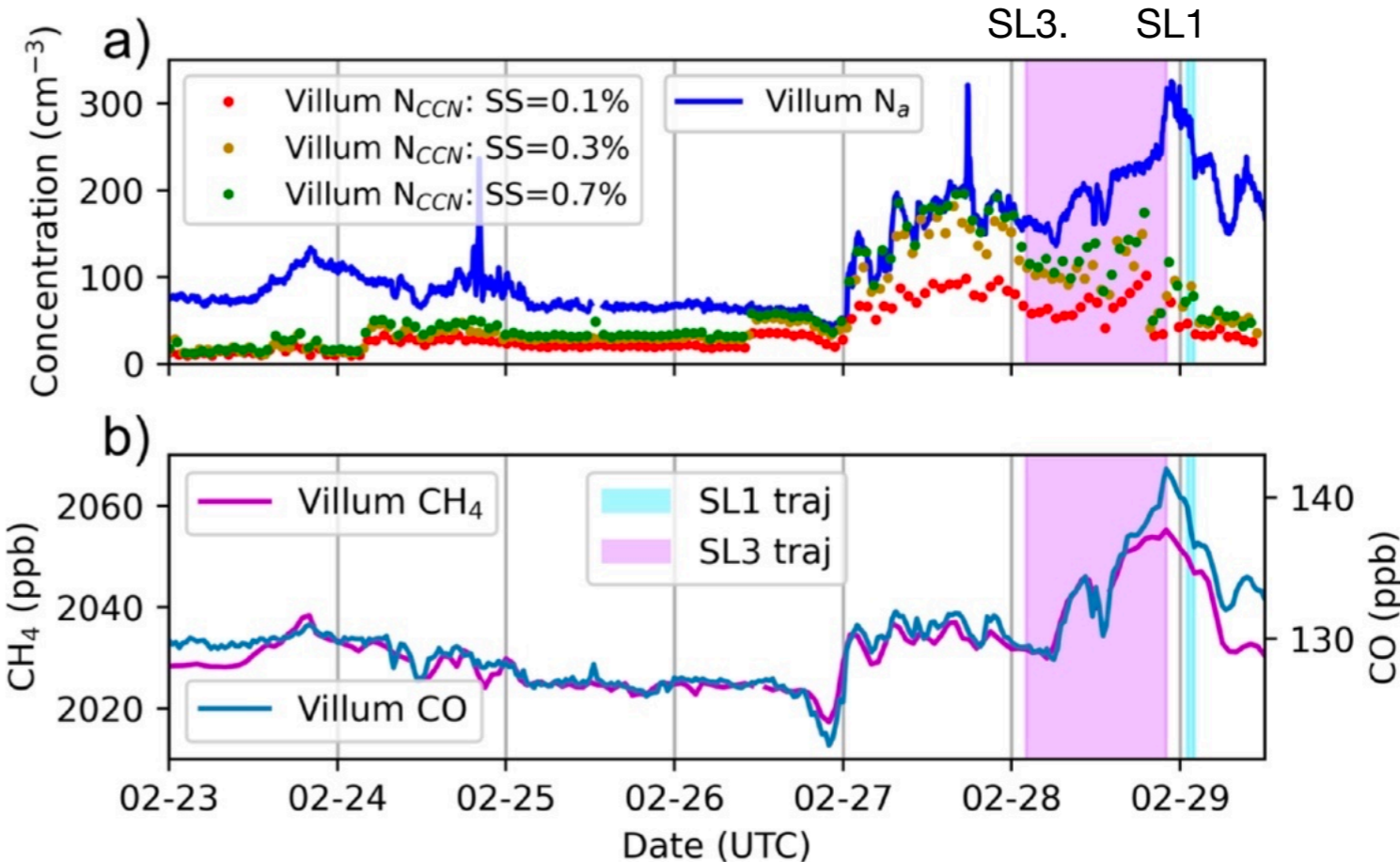
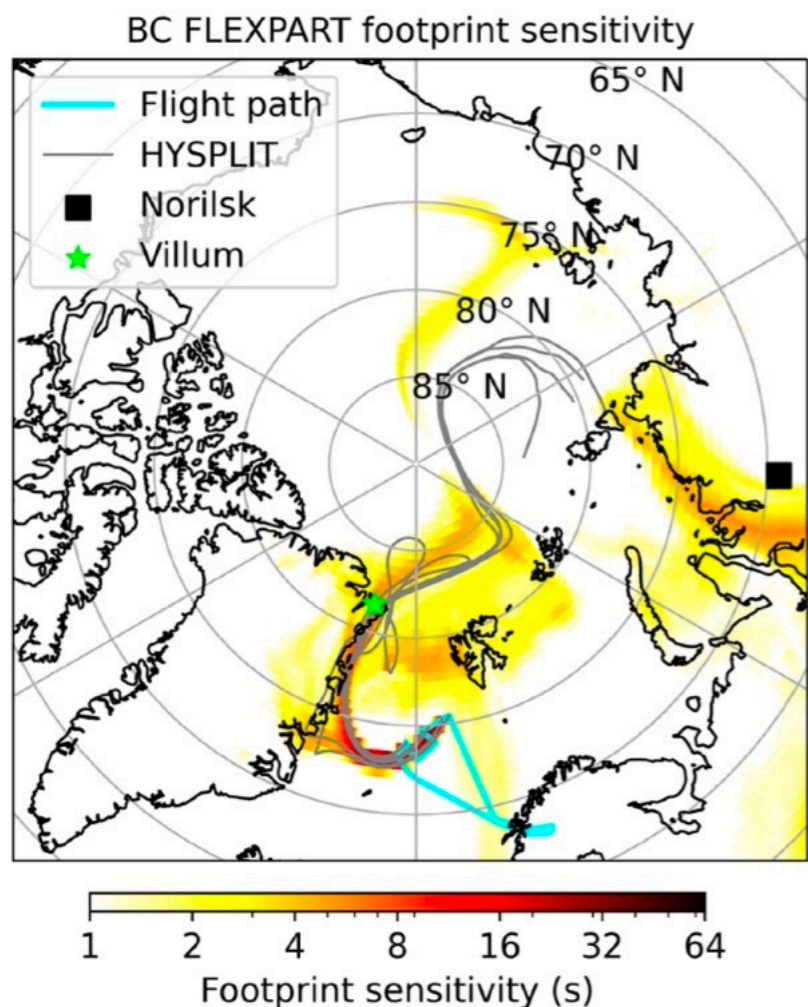


Newman, E., B. Geerts, J. D. Doyle, C. Grasmick, P. Zuidema, S. Ephraim, and Z. Wang, 2025: Airborne observations of the vertical structure of a shallow polar low in the Norwegian Sea. *Mon. Wea. Rev.*, **154**, <https://doi.org/10.1175/MWR-D-25-0109.1>.

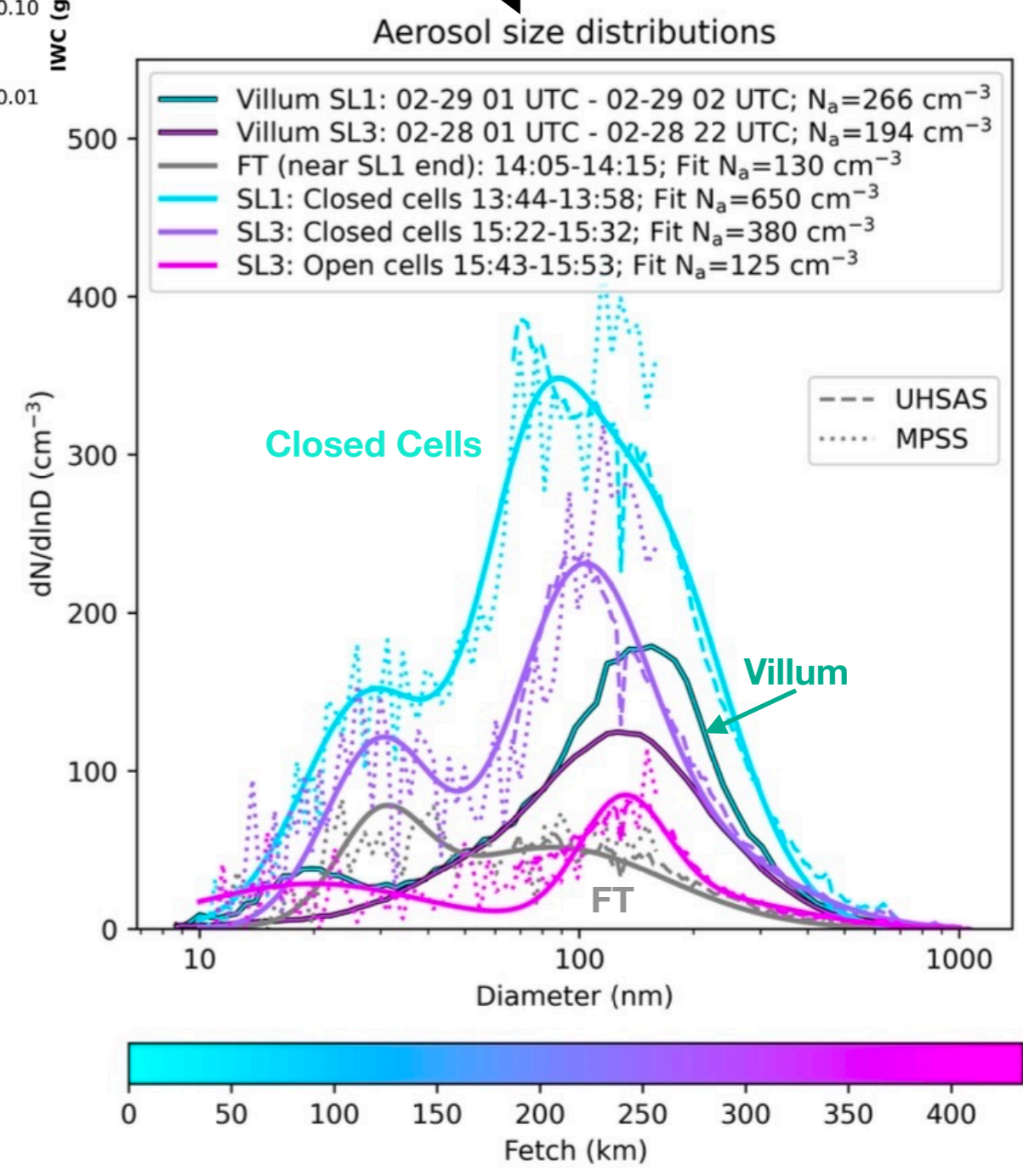
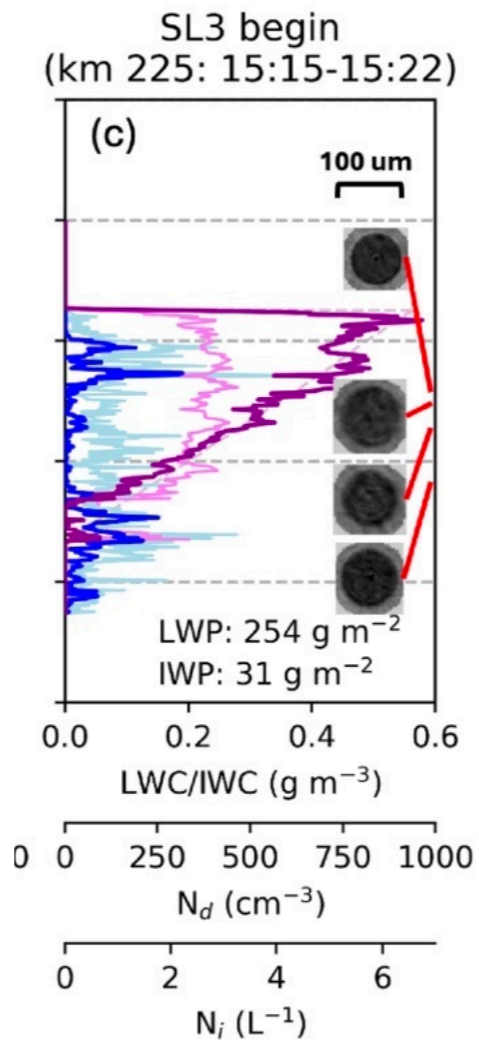
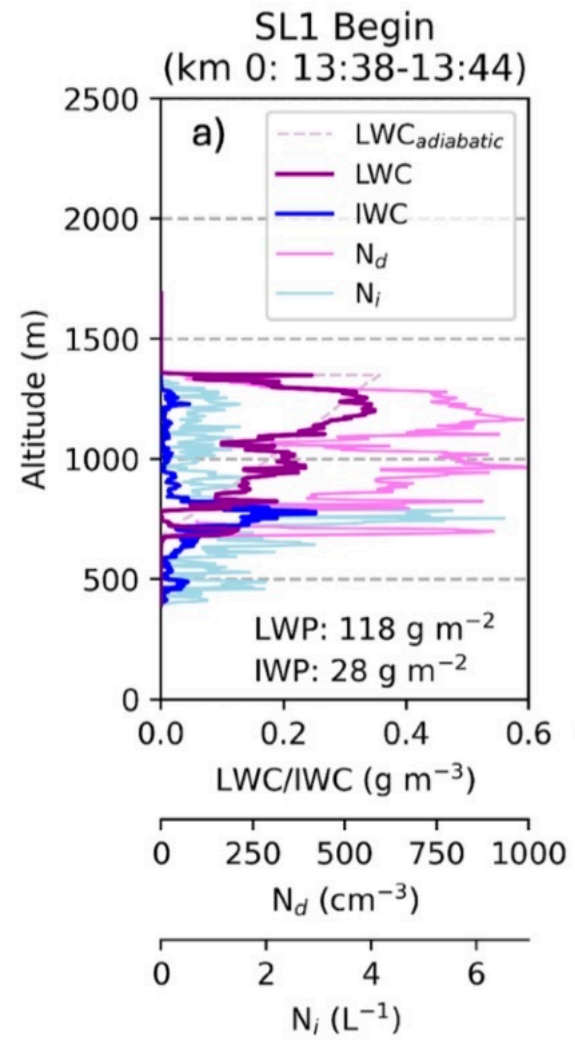
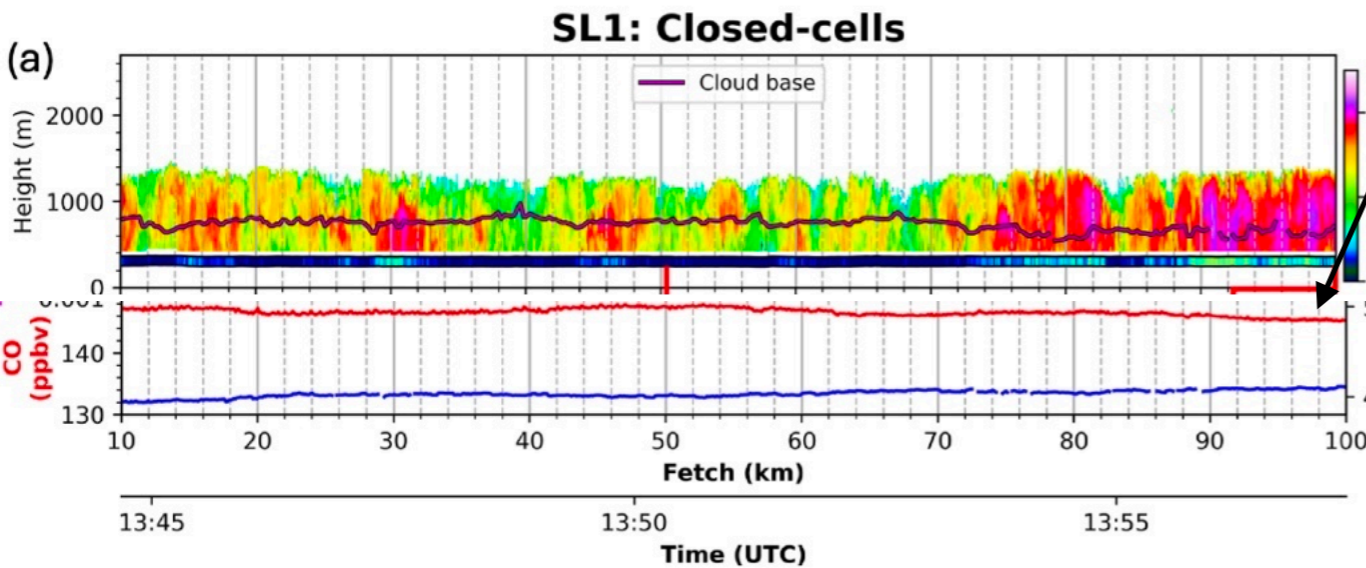


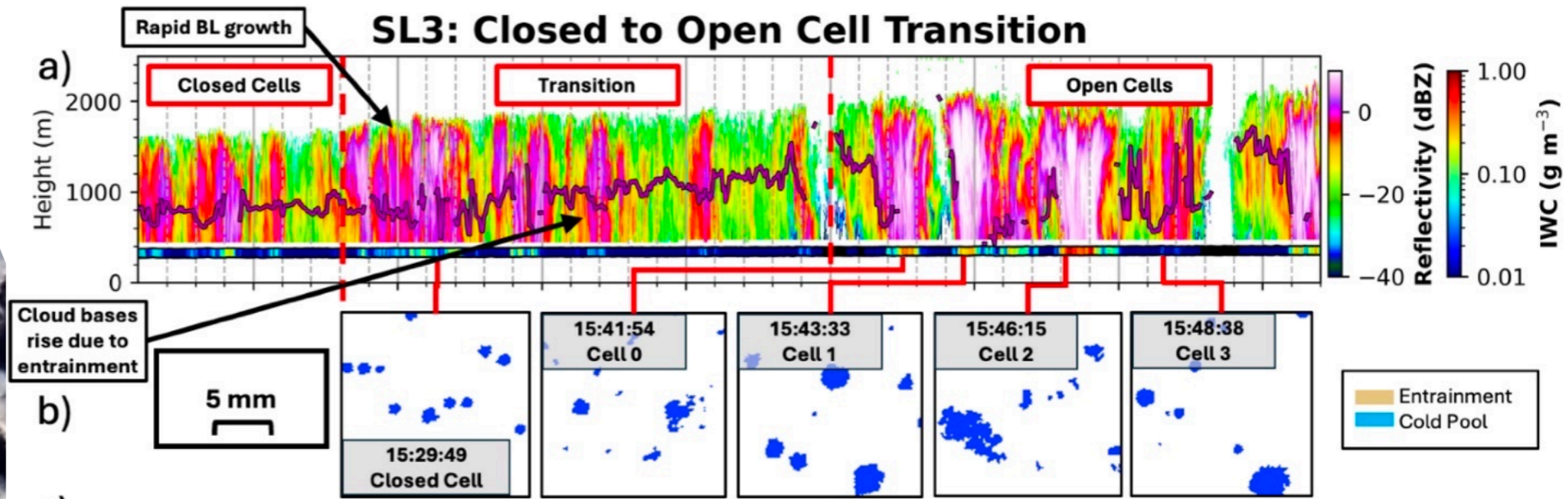
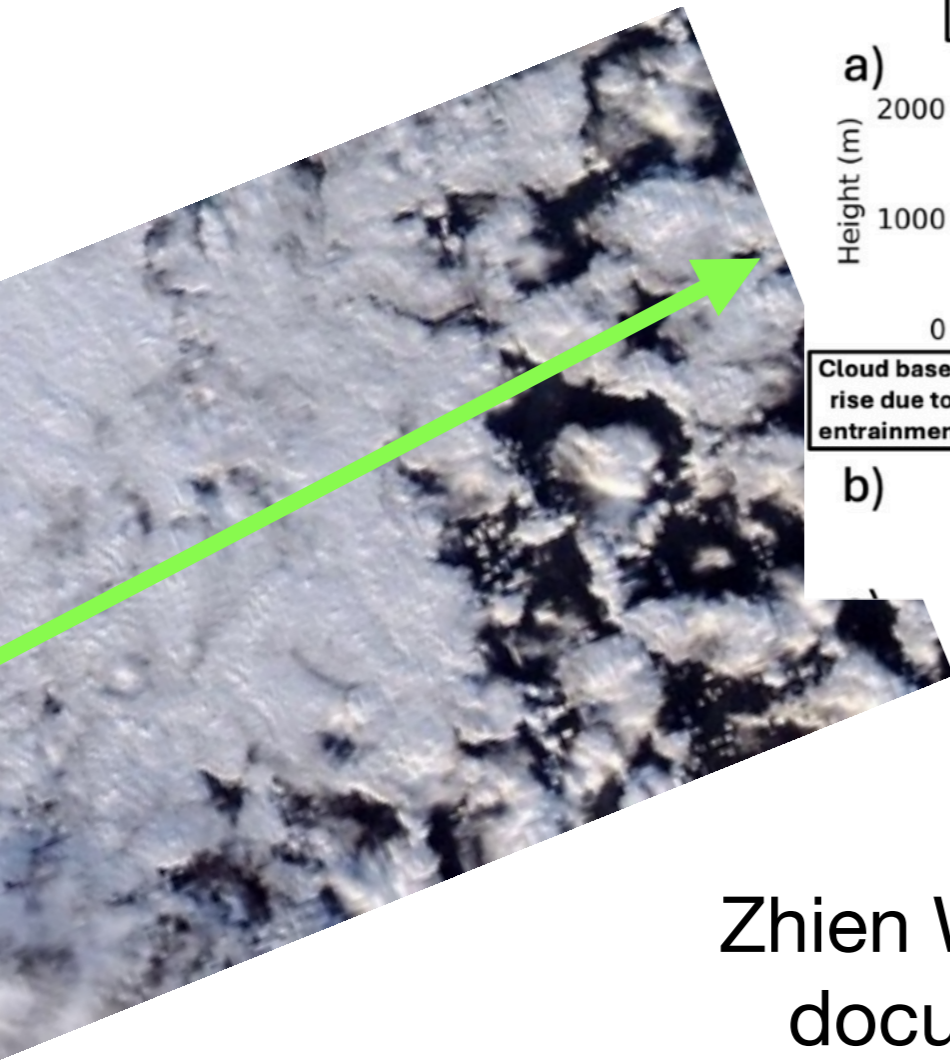


Back-trajectories flow past Villum Research Station northeast Greenland; corroborate pollution advected in from Norilsk, Siberia

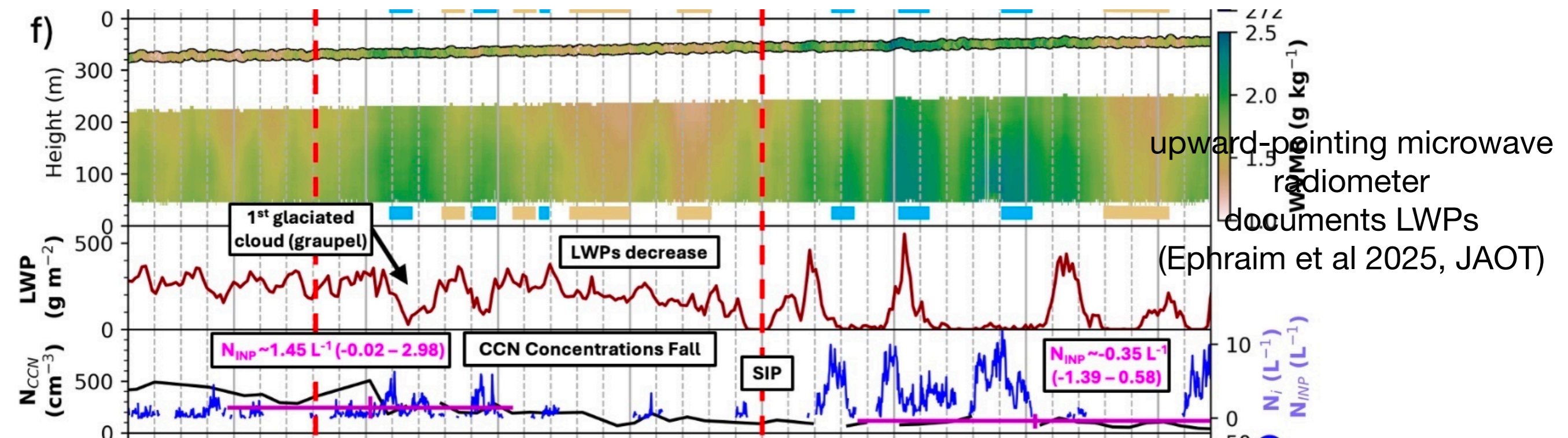


Closed-cell aerosol size distribution is bimodal (accumulation+Aitken aerosol). Villum is mostly accumulation-mode aerosol, free-troposphere aerosol is dominated by Aitken aerosol. *An entrainment estimate based on CO & O3 suggests free-tropospheric entrainment primarily dilutes the boundary-layer accumulation-mode aerosol (precipitation is < 0.5 mm/hr) increasing the droplet effective diameter*





Zhien Wang's downward-pointing Raman lidar documents cold pools/entrainment events



Liquid-producing (f) updrafts (b) associated with reduced wind speeds (a) indicating surface wind convergence.

Cold pools located to the east (right) of the updrafts (advected with mean winds)

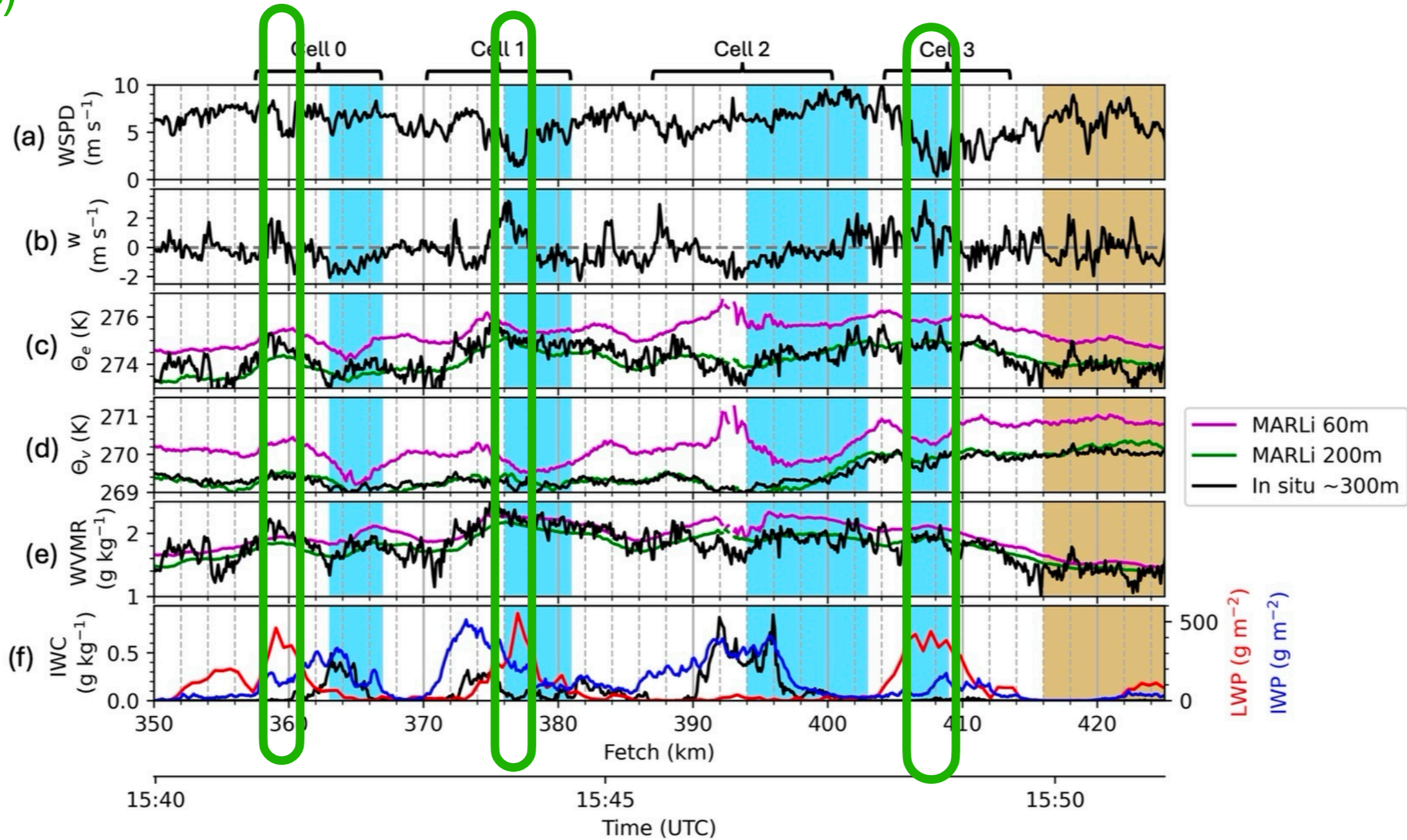


Figure 16. In situ flight level (300 m) (a) horizontal wind speed (WSPD) and (b) vertical wind velocity (w), (c) Θ_e , (d) Θ_v , and (e) WVMR. c-e) also include MARLi-derived values at 60 m and 200 m altitude. (f) Retrieved LWP/IWP and in-situ IWC. From km 391 (15:46:06 UTC) to km 394 (15:46:33 UTC), the lowest level MARLi derived parameters (θ_e , θ_v , and WVMR; are impacted by heavy ice precipitation attenuating the MARLi signal.

Left side of cold pools is where the liquid will be

Right side of cold pools is its extension

Prevailing
Wind

RCM1 SAR wind 16:34 UTC

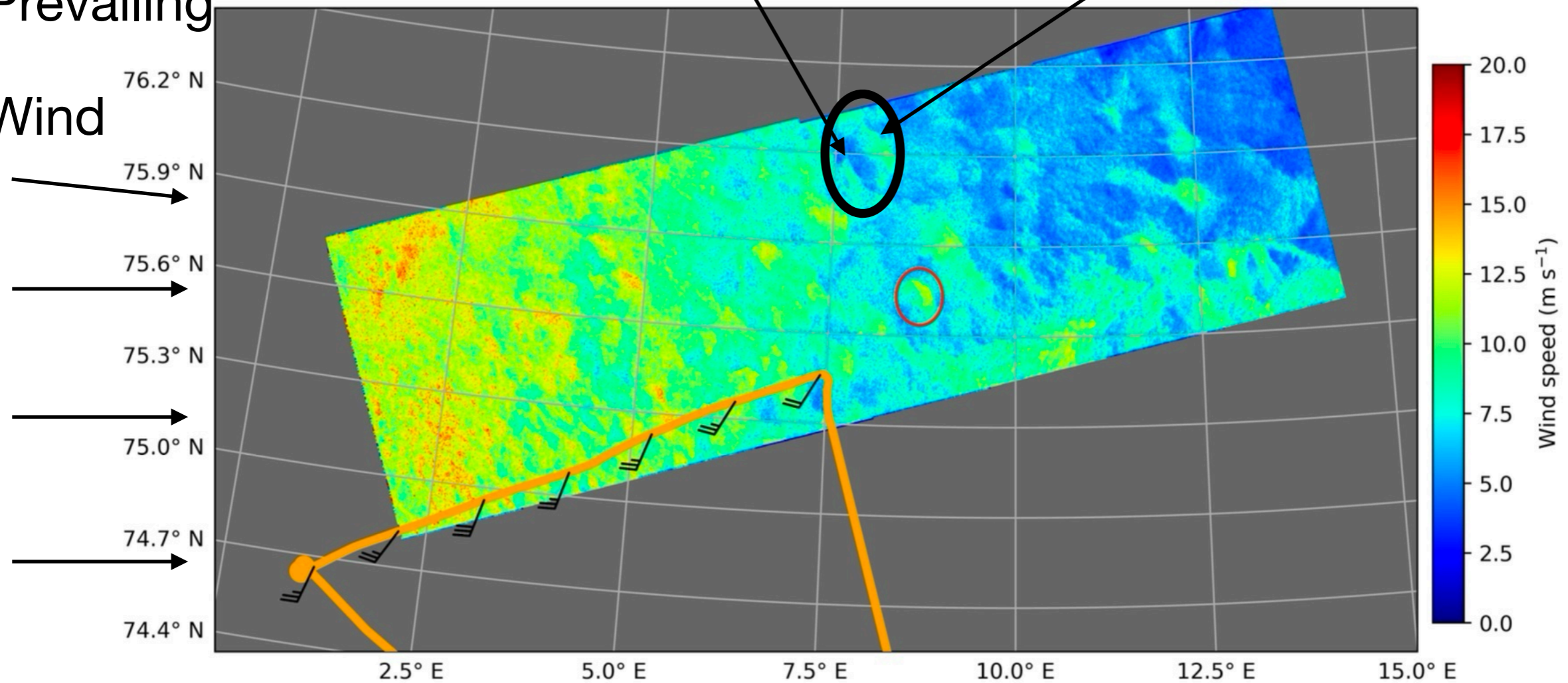


Figure 15. SAR imagery from RadarSat Constellation Mission 1 (RCM1) showing the 10 m wind field in the vicinity of SL3 ~30 minutes after the completion of SL3. Flight track is overlaid on the wind field along with flight-level (300 m) wind barbs (knots). An example of a cold pool signature is circled. at 75°N, 1° longitude is approximately 29 km.

Cold pools in RF02 too weak to thermodynamically decouple the sub-cloud atmosphere. Buoyancy fluxes $\sim 200\text{-}250 \text{ W m}^{-2}$! Cold pools seem to most just organize where the warm, moist plumes draft up

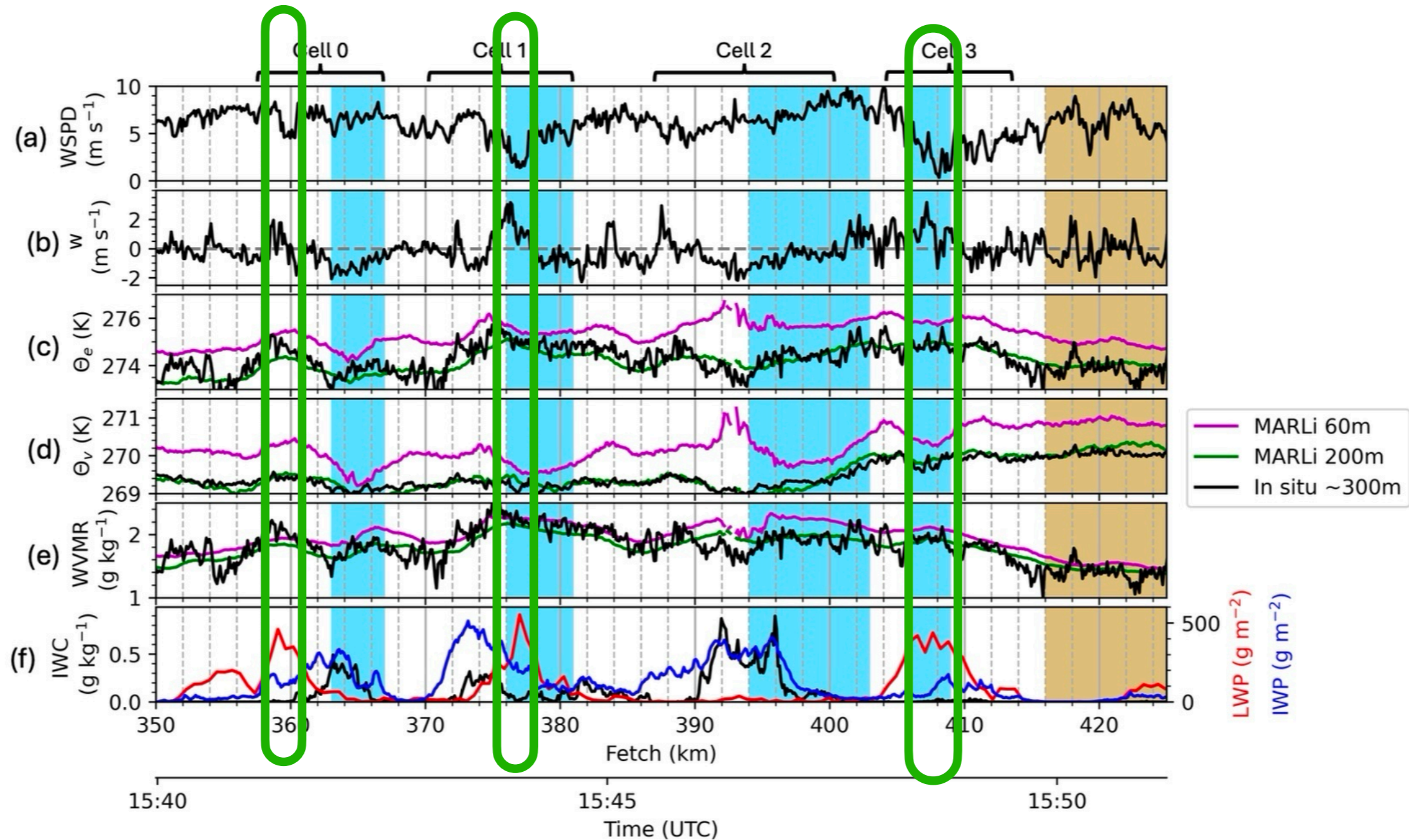
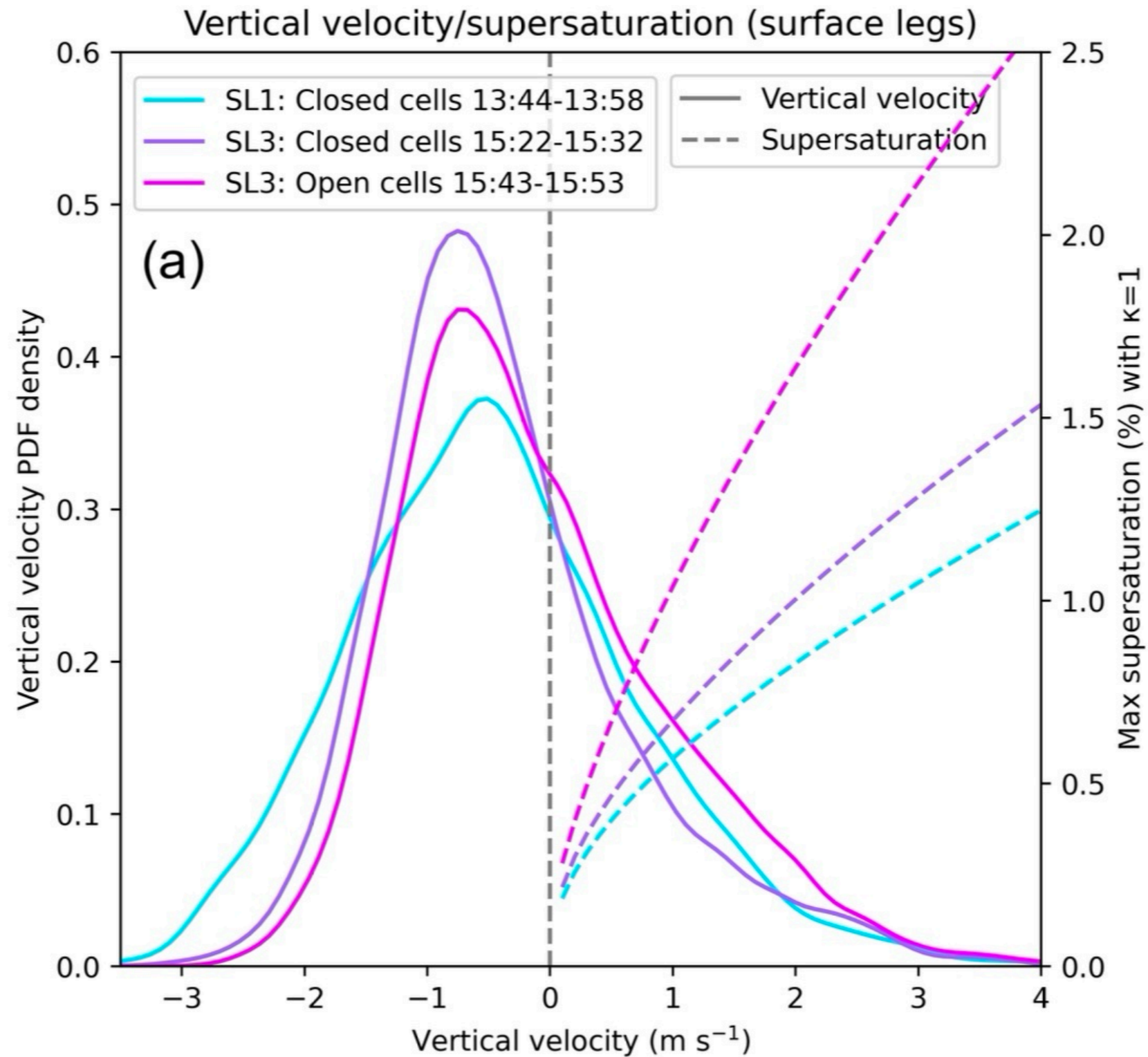


Figure 16. In situ flight level (300 m) (a) horizontal wind speed (WSPD) and (b) vertical wind velocity (w), (c) Θ_e , (d) Θ_v , and (e) WVMR. c)-e) also include MARLi-derived values at 60 m and 200 m altitude. (f) Retrieved LWP/IWP and in-situ IWC. From km 391 (15:46:06 UTC) to km 394 (15:46:33 UTC), the lowest level MARLi derived parameters (θ_e , θ_v , and WVMR; are impacted by heavy ice precipitation attenuating the MARLi signal.

Vertical velocity distribution is positively-skewed, along with overcast 'stratocumulus'-like cloud deck



CAESAR-related talks/posters at AMS Madison

Monday August 3:

3pm-4:30 posters

Sam Ephraim et al.: A Closed to Open-Celled Mixed-Phase Cloud Transition Observed Over the Nordic Seas Under High Aerosol Loading.

Xia et al.: Marine Boundary Layer Cloud Evolution along an Arctic Cold Air Outbreak: Results from CAESAR Airborne Observations and Simulations

Wednesday August 5:

Marine Cold Air Outbreaks Joint Session 9 8:30-10:00

9:15am Cai et al.: Aerosol Scavenging in Arctic Marine Stratocumulus Clouds during Cold Air Outbreaks

9:30 am An Yang et al.: Cloud and Precipitation Evolution and the Role of Sublimation in Arctic Marine Cold-Air Outbreaks from CAESAR

3pm-4:30 posters

Pablo Velt et al.: Understanding the Transition from Shallow to Deep Open-Cellular Convection In a Marine Cold Air Outbreak: A Case Study from CAESAR

Zhien Wang et al.: Quantify Ice Generation of Cold Air Outbreak Clouds with Combined Airborne Lidar and Radar Observations

Bailey et al: Tracing the Isotopic Signature of Extreme CAO Evaporation In Precipitation

Thursday August 6:

3pm-4:30 posters

Martrich et al.: Assessing the Spatial Scales Resolved by High-Rate Nevzorov Hot-Wire Probe Measurements During CAESAR

Community Engagement Is Important to NSF campaigns



edec.ucar.edu/public/field-projects/caesar

The Science of CAESAR



Official Selection
Polar Film Fest
2024

NCAR
UCAR

The Science of CAESAR



Watch later



Share

Climate change • Climate change refers to long-term shifts in temperatures and...

THE SCIENCE OF CAESAR



Watch on YouTube

Data publicly available, some value-added products still under development

Product	Description	doi
aerosol	CN+SMPS+UHSAS+SP2+PCASP	10.26023/DQFV-MKGR-J608
microphysical	merged 2D-S+HVPS3, 2D-S liquid/ice discrimination	tbd
remote sensing	merged WCR+WCL+KPR+MARLi,WCL-cloud top,base heights	10.26023/9SGP-MXGP-MA06
camera movies+animated plots	z,p,lon,temp,w,LWC,N _{2DS} , N _{CDP} ,O ₃ ; MP4, RF 4,5,6,9,10 only	10.26023/NKZO-AXTJ-TF08

www.eol.ucar.edu/field_projects/caesar

67%

NSF | NCAR

Contact Us Search EOL

Earth Observing Laboratory

Who We Are Platforms & Instruments Field Programs Our Services Data & Software Research & Development News & Events

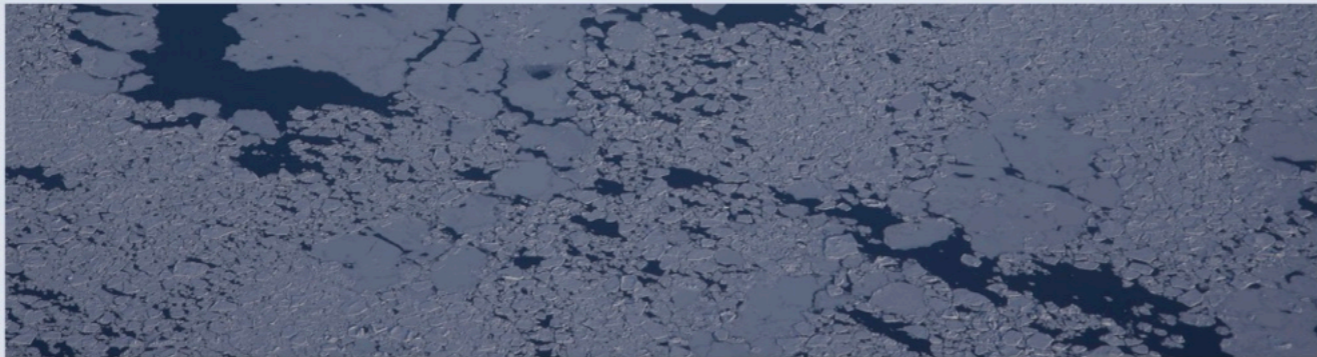
Home / CAESAR

CAESAR

Cold Air Outbreak Experiment in the Sub-Arctic Region

PROJECT DATES: 02/22/2024 - 04/07/2024
PROJECT LOCATION: Kiruna, Sweden

PROJECT DESCRIPTION



Why It Matters - Cold-air outbreaks can lead to severe weather at both high and mid-latitudes, impact global weather patterns, and cause direct consequences for human

CAESAR Publications

CAESAR Publications

Data Access

CAESAR Data Access

Field Catalog

CAESAR Field Catalog

CAESAR Data Documentation

CAESAR Project Manager Report
 CAESAR Data Submission Instructions
 CAESAR Data Policy
 Dataset Documentation
 Requirements
 EOL Data Policy
 DOI Guidance for Authors
 List of Aircraft Variables
 CAESAR 2023 Dry Run

Discussion to request C-130 for CAO-focused “MORPHEUS” project out of Maine, spring 2028....ability for NSF to consider this is not promising

